Specialty Journal of Pharmacognosy, Phytochemistry, and Biotechnology
ISSN: 3062-441X
2023, Volume 3, Page No: 93-115

Available online at: www.galaxypub.co/page/journals

Galaxy Publication

Galaxy Publication

Paromomycin Inhibits HDAC1-Dependent SUMOylation and IGF1R Membrane Translocation in Glioblastoma

Sarah Mitchell[1]*, Olivia Brown[1], James Walker[1]

[1]Department of Pharmacognosy, School of Pharmacy, University of Sydney, Sydney, Australia.

***E-mail** ✉ sarah.mitchell.pg@outlook.com

Received: 09 January 2023; **Revised:** 23 March 2023; **Accepted:** 25 March 2023

ABSTRACT

This work explores how Paromomycin influences SUMOylation-associated signaling in glioblastoma (GBM), with a particular focus on its inhibitory action on HDAC1. SUMOylation-related genes linked to GBM outcomes were screened using TCGA and GTEx datasets. Molecular docking predicted Paromomycin as a likely HDAC1 inhibitor. Functional experiments in U-251MG GBM cells—including CCK8 viability assays, qRT-PCR, and immunofluorescence—were conducted to evaluate its impact on SUMOylation gene activity, cell growth, and IGF1R trafficking. Paromomycin reduced GBM cell survival, colony formation, and migratory capacity in a concentration-dependent manner. It altered SUMO1 expression and suppressed IGF1R entry into the nucleus, an effect counteracted by the HDAC1 inhibitor Trichostatin A (TSA), supporting a role for Paromomycin in SUMO1-dependent regulatory mechanisms. These findings position Paromomycin as a promising GBM therapeutic candidate through its modulation of HDAC1-driven SUMOylation processes and regulation of IGF1R nuclear transport, emphasizing the need for further clinical-oriented studies.

Keywords: Drug screening, Paromomycin, Glioblastoma multiforme, HDAC1, IGF1R, SUMOylation

How to Cite This Article: Mitchell S, Brown O, Walker J. Paromomycin Inhibits HDAC1-Dependent SUMOylation and IGF1R Membrane Translocation in Glioblastoma. J Pharmacogn Phytochem Biotechnol. 2023;3:93-115. https://doi.org/10.51847/ZlSy1ptrQD

Introduction

Glioblastoma Multiforme (GBM) represents the most severe and fast-progressing primary brain malignancy in adults, typically arising within the central nervous system [1, 2]. Its rapid clinical deterioration, pronounced invasiveness, and poor response to conventional therapeutic approaches impose significant physical and emotional strain on patients and caregivers [3, 4]. Comprising nearly half of all primary brain tumors, GBM stands as the most frequently diagnosed malignant brain tumor among adults, with incidence peaking in middle-aged and older populations [5-8]. Incidence patterns additionally demonstrate a modest male predominance and higher rates within specific demographic groups, including African Americans [9]. This tumor type is linked to substantial mortality, requiring multimodal and resource-intensive interventions—neurosurgical procedures, radiotherapy, chemotherapy, and long-term rehabilitative support [10-12]. Such complexities highlight the urgent need to deepen our understanding of GBM biology and accelerate the development of more effective therapeutic options. The pronounced heterogeneity of GBM is driven by diverse molecular abnormalities, including gene mutations, chromosomal instability, and suppression of tumor-inhibitory pathways [13, 14]. These genetic alterations shape tumor initiation, progression, and treatment resistance [15, 16]. Compromise of the blood–brain barrier (BBB) further promotes tumor infiltration and simultaneously restricts adequate drug penetration. Although standard management relies on surgical resection followed by radiotherapy and chemotherapy, tumor recurrence—often multifocal—is common due to incomplete resection and acquired resistance to cytotoxic therapies. Median survival remains limited to approximately 12–15 months after diagnosis, with outcomes varying based on individual clinical factors. These realities reinforce the necessity of identifying novel intervention pathways that may improve therapeutic success. Experimental observations demonstrate that biochemical modulation and

environmental stimuli can elicit diverse cellular responses, revealing several promising therapeutic targets across different research settings [17-19].

The integration of pharmacological research with computational biology continues to advance medical innovation, with large-scale bioinformatics resources providing insights into long-term health trends and facilitating evidence-based clinical decisions [20-26]. In parallel, disease-relevant animal models remain indispensable for validating drug efficacy and generating rigorous translational data [27, 28]. Within clinical settings, shared decision-making frameworks and structured checklists have increased patient satisfaction and involvement in treatment selection [29, 30]. Meanwhile, rapid advancements in artificial intelligence (AI) are transforming modern medicine by enhancing diagnostic accuracy and enabling personalized therapeutic recommendations [31, 32].

Approaches focused on gene–environment interactions, a key branch of bioinformatics, have enabled the interpretation of survival patterns based on extensive genomic datasets and have uncovered molecular networks underlying complex disorders [33]. The combined progress of bioinformatics and molecular science has dramatically expanded current knowledge of GBM through multi-omics analyses, thereby opening pathways for emerging therapeutic modalities [34, 35]. Current research is increasingly centered on individualized treatment, targeted molecular interventions, and immunotherapy strategies designed to overcome radioresistance and improve clinical outcomes [36, 37]. An integrated understanding of GBM's epidemiology, pathology, and therapeutic limitations is necessary to refine treatment modalities [38, 39]. Future studies should continue to prioritize the exploration of molecular drivers of tumor development and therapeutic resistance, with the aim of converting these discoveries into improved survival and enhanced patient quality of life [40, 41].

Among promising therapeutic avenues, post-translational modifications (PTMs) — particularly SUMOylation (Small Ubiquitin-like Modifier modification) — have emerged as influential regulators of tumor biology [42, 43]. SUMOylation governs essential cellular processes such as cell-cycle progression, DNA damage repair, and programmed cell death [44]. Growing evidence indicates that heightened SUMOylation activity can accelerate GBM initiation and progression by affecting these regulatory pathways, positioning this modification as a compelling therapeutic target [45].

At the genomic level, numerous studies have established strong associations between genetic alterations and GBM onset and evolution [46, 47]. Identification of novel biomarkers and molecularly guided therapies continues to open new directions for GBM treatment [48]. Mutations in IDH1/IDH2, for example, are frequently observed in GBM and are linked to metabolic shifts that influence tumor growth and survival [49, 50]. Likewise, disruptions or deletions in TP53 impair p53-mediated regulatory mechanisms, destabilizing cell-cycle control and DNA repair processes [51, 52]. These molecular abnormalities not only aid in GBM diagnosis and classification but also represent potential intervention points [53].

Advances in bioinformatics have transformed approaches to disease investigation, enabling multi-omics integration that reveals fundamental mechanisms behind disease progression [54-58]. Such comprehensive analyses now play central roles in diagnostic refinement, prognostic evaluation, and therapeutic decision-making, reinforcing the principles of precision medicine [59-64].

The present study investigates the influence of Paromomycin on SUMOylation-associated pathways in GBM. By integrating bioinformatics approaches, molecular docking, and in-vitro experimentation, this research aims to support the development of refined targeted strategies for GBM management.

Materials and Methods

Expression profiling of SUMOylation-related genes in pan-cancer datasets

This study systematically evaluated the expression of SUMOylation-related genes across diverse cancer types. Differences in gene expression between malignant tissues and matched non-tumor controls were examined using the Wilcoxon Rank Sum Test. For paired analyses comparing tumor samples with their adjacent non-tumor counterparts within each cancer type, the Wilcoxon Signed Rank Test was applied. TPM-normalized expression profiles from GTEx normal tissues were merged with TCGA tumor datasets using the tcgasandbox_RSEM_gene_tpm and gtexsandbox_RSEM_gene_tpm resources available through the UCSC Xena platform. After merging, all data were converted to Z-scores to ensure consistency and comparability among tumor subtypes.

For analyses specifically focused on GBM, we again employed the Wilcoxon Rank Sum Test to compare differences between tumor and non-tumor tissue expression. As a non-parametric approach commonly used to

test median differences between independent groups, this method allowed evaluation of gene-expression variation at an $\alpha = 0.05$ significance threshold.

Promoter methylation assessment of SUMOylation-related genes

Methylation analyses targeted several regulatory genomic regions, including TSS1500 (200–1,500 bp upstream of the TSS), TSS200 (within 200 bp of the TSS), the first exon, and the 5′UTR. Median methylation levels were calculated across these regions for each sample to estimate cumulative promoter-associated methylation. A Spearman correlation analysis — chosen for its non-parametric nature and lack of assumptions regarding variable distribution — was performed to determine associations between methylation levels (independent variable) and gene-expression levels (dependent variable). Group-level methylation differences between tumor and non-tumor samples were further assessed using the Wilcoxon Rank Sum Test to evaluate distributional shifts between independent sample sets.

ATAC-seq analysis of SUMOylation-related genes

ATAC-seq signals associated with SUMOylation-related genes were analyzed using the ChIPseeker package in R. Peaks were annotated relative to transcription start sites (TSS) using the parameter tssRegion = c(−3,000, 3,000), encompassing a region extending 3 kb upstream and 3 kb downstream of the TSS. This window captures regulatory elements involved in transcriptional activation, including transcription-factor binding and histone-modification sites. Chromosomal peak distributions were visualized using the covplot function, allowing mapping of peak density, genomic location, and cancer-type associations across chromosomes.

Genomic characterization of SUMOylation-related genes in pan-cancer studies

Copy number variation (CNV) and DNA methylation datasets from TCGA were compiled across multiple tumor types, arranging samples as matrix rows and genes or genomic loci as columns, followed by routine preprocessing steps to eliminate poor-quality entries and adjust for technical variability. In OSCC datasets, CNV profiling was carried out using GISTIC and CNAnorm, enabling classification of SUMOylation-related genes into amplified or deleted categories based on their CNV signatures. Promoter methylation levels for these genes were evaluated in tumor versus normal tissues via the UALCAN platform, and broader methylation tendencies across cancers were examined through MethSurv to explore links between epigenetic states and cancer prevalence. Mutation Annotation Files (MAF) were retrieved from TCGA using the "TCGAbiolinks" R package, and tumor mutation burden (TMB)—a marker of genomic instability and a potential predictor of immunotherapy responsiveness—was computed with "maftool." Correlation analyses, survival assessments, and additional computational techniques in R were employed to investigate how SUMOylation-related gene expression corresponds with CNV alterations, methylation dynamics, TMB variability, tumor behavior, and clinical outcomes.

GSEA enrichment analysis across pan-cancer types

RNA-seq and microarray datasets representing both malignant and adjacent normal tissues were sourced from TCGA and preprocessed to remove low-quality samples and unreliable probes. Differential gene expression was evaluated using the "limma" package, which incorporates normalization, background correction, and statistical modeling to detect significantly altered genes. Genes meeting established log2 fold-change (log2FC) and P-value thresholds were retained as key findings. Gene Set Enrichment Analysis (GSEA)—implemented with the "clusterProfiler" package—was used to interpret these differential patterns through KEGG, GO, and Reactome pathway frameworks. Enrichment Scores (ES), which quantify the strength of association between gene expression and biological pathways, facilitated the prioritization of relevant functional categories. Visual representations—including bar charts, heatmaps, and scatter plots—were created using "ggplot2," allowing flexible and detailed illustration of enriched pathways and expression trends.

Tumor prognosis analysis

Using clinical metadata alongside RNA-seq and microarray datasets from TCGA, we evaluated how dysregulated SUMOylation-related genes might influence patient overall survival (OS). Differential expression was again assessed using the "limma" package, helping identify genes exhibiting significant tumor-associated shifts. To examine prognostic relevance, Cox proportional hazards modeling was performed via the "survival" package, and Kaplan–Meier survival distributions were constructed to compare OS between high- and low-expression groups.

Statistical significance in survival differences was tested using the log-rank method, and graphical outputs were generated using "survminer" for enhanced visualization of survival trajectories.

Developing a prognostic model for SUMOylation-related genes in GBM

To assess the diagnostic capability of the ssGSEAscore in distinguishing tumor from normal tissue, ROC curve analysis was conducted with the "pROC" package, reporting the AUC along with a smoothed ROC curve and 95% confidence band. ssGSEAscores were computed using the "gsva" package with the single-sample GSEA (ssgsea) algorithm. Expression data were obtained from the EBPlusPlusAdjustPANCAN_IlluminaHiSeq_RNASeqV2 dataset within the PanCanAtlas collection (geneExp.tsv), which was processed using the Firehose pipeline with MapSplice and RSEM, and normalized by setting the upper quartile value to 1,000. Comparisons of ssGSEAscore values between tumor and non-tumor tissues in GBM were performed using the Wilcoxon Rank Sum Test, while tumor versus adjacent-normal comparisons used the Wilcoxon Signed Rank Test. Model accuracy and calibration were evaluated through calibration curves and goodness-of-fit metrics. Additionally, changes in ssGSEAscore across GBM stages were examined using the Wilcoxon Rank Sum Test, and differences across multiple GBM progression categories were analyzed via the Kruskal–Wallis Rank Sum Test.

Survival prognosis analysis of SUMOylation-related genes in GBM using ssGSEA

To clarify how SUMOylation-associated signatures relate to patient outcomes in glioblastoma, enrichment values obtained from ssGSEA were incorporated into several survival models. Using the survival ecosystem in R, we generated survival curves for overall survival (OS), disease-specific survival (DSS), and progression-free interval (PFI). Group separation was established with the survminer package, which selected a cutoff ensuring that no survival group was reduced below a 0.3 ratio. The survfit procedure produced the survival estimates, and intergroup differences were examined through log-rank comparison.

A broader view was obtained by subjecting sixteen eligible datasets to a Cox-based meta-analytic approach, with inverse-variance principles applied to log-transformed hazard ratios (HRs). HR values below 1 were interpreted as reflecting potential tumor-restraining activity, whereas values above 1 hinted at tumor-promoting behavior; however, this binary frame was not sufficient to encompass the wide regulatory scope of SUMOylation-related genes. All integrative statistics and visualization procedures were implemented in R (version 4.3.2) using the Meta package.

Each gene was further examined individually through univariate Cox modeling using the coxph() function, and the corresponding HR estimates with 95% confidence intervals (CIs) were summarized in forest plots generated with the forestplot package.

Core protein drug sensitivity screening

To explore potential pharmacological agents targeting the core proteins of interest, we relied on an in silico screening strategy. Three-dimensional conformations for 321 FDA-approved compounds were retrieved from the ZINC repository, and the relevant protein domains were obtained as PDB files from the Protein Data Bank. The Libdock module in Discovery Studio 2019 (DS 2019) served as the computational engine for docking.

Before docking simulations, receptor structures were refined by eliminating water molecules, optimizing overall geometry, and applying energy minimization routines to both protein and ligand structures. Critical residues were assigned appropriate ionization states; possible tautomeric variants were generated; non-polar hydrogens were removed; and Gasteiger–Marsili partial charges were applied. Docking runs assessed the compatibility of each compound with predicted binding pockets on the target proteins, generating interaction profiles that provide a foundation for subsequent structural optimization and experimental confirmation.

CCK8 proliferation activity assay

To evaluate growth responses to Paromomycin, U-251MG cells were plated at 5×10^3 cells per well in 96-well plates and exposed to defined drug concentrations for 48 h. After exposure, 10 μL of CCK-8 reagent was added to each well, followed by a 2-h incubation period prior to measuring absorbance at 450 nm. For TSA assessment, cells received fresh medium containing 100 nM TSA for 24 h, with 0.1% DMSO serving as the vehicle control. All proliferation experiments were performed in triplicate.

qRT-PCR

Total RNA extraction began by adding 1 mL of Trizol to each well, transferring the lysate to microtubes, and allowing a 10-min lysis period. Samples then underwent sonication, after which 200 μL chloroform was mixed in and centrifuged at 12,000 rpm for 15 min at 4°C. The aqueous layer was isolated, combined with 400 μL isopropanol, and centrifuged to precipitate RNA. The resulting pellet was dissolved in 20 μL of DEPC-treated water. Reverse transcription was conducted under the specified thermal program, and the synthesized cDNA was used for qRT-PCR quantification.

Immunofluorescence

Slides containing cultured cells were processed by incubating them in BSA for 1 h to block nonspecific interactions. Following rinsing, the slides were placed in primary antibody solutions overnight at 4°C: anti-CAS3 diluted 1:250 or anti-SUMO1 diluted 1:100. On the next day, slides were washed in PBS and then incubated with a fluorescein-conjugated secondary antibody for 2 h at room temperature. After nuclear staining with DAPI and final washing steps, slides were fixed and visualized under a fluorescence microscope to assess CAS3 and SUMO1 expression patterns across different cellular regions.

Colony formation assay for U-251MG cells

To determine longer-term growth potential following Paromomycin exposure, U-251MG cells were maintained in DMEM (Gibco BRL, MD, United States) supplemented with 10% FBS (HyClone). Cells were seeded at 500 cells per well in six-well plates and allowed to adhere before drug treatment. Paromomycin or DMSO control was then applied, with treatment medium refreshed every 3–4 days. After a 10–14-day growth period, once colonies became evident, cultures were gently washed with PBS, fixed in 4% paraformaldehyde for 15 min, stained with 0.5% crystal violet for 20 min, rinsed in distilled water, and left to dry for later quantification.

Statistical analyses

All statistical computations were conducted using GraphPad Prism 8.0 (GraphPad Software, La Jolla, CA, USA). Experiments were performed in triplicate to ensure reproducibility, and results are presented as mean ± standard deviation (SD). For comparisons between two groups, a two-tailed Student's t-test was applied. Data normality was evaluated using the Shapiro-Wilk test, and homogeneity of variances was assessed with Levene's test. When comparisons involved more than two groups, one-way analysis of variance (ANOVA) was conducted, followed by Tukey's post hoc test to identify pairwise differences. Statistical significance was defined as a p-value ≤ 0.05.

Relationship between SUMOylation-related gene expression and tumor prognosis

We examined the impact of ten SUMOylation-associated genes (HDAC1, HDAC4, HDAC9, PIAS1, PIAS2, RAN, RANBP2, SUMO1, RANGAP1, and SUMO1) on overall survival (OS) across multiple cancer types **(Figure 1)**. Forest plots illustrate hazard ratios (HRs) with 95% confidence intervals (CIs) for each gene in different malignancies.

High HDAC1 expression was consistently associated with poorer OS and elevated risk in several cancers **(Figure 1a)**. HDAC4 exhibited a similarly strong prognostic value, with elevated expression linked to unfavorable outcomes **(Figure 1b)**. HDAC6 followed the same trend, as demonstrated in **Figures 1c and 1d**, showing a clear correlation with reduced survival. PIAS1 **(Figure 1e)** and PIAS2 **(Figure 1f)** displayed variable prognostic effects, indicating that their influence may differ depending on the cancer type. Elevated RAN levels were correlated with decreased OS **(Figure 1g)**, whereas higher expression of RANBP2 **(Figure 1h)** and RANGAP1 **(Figure 1i)** appeared protective, associated with improved survival. SUMO1 **(Figure 1j)** demonstrated context-dependent effects, acting as either a risk or protective factor depending on the malignancy examined.

Collectively, these findings highlight the prognostic relevance of SUMOylation-related genes and suggest their potential utility as both predictive biomarkers and therapeutic targets across diverse cancer types.

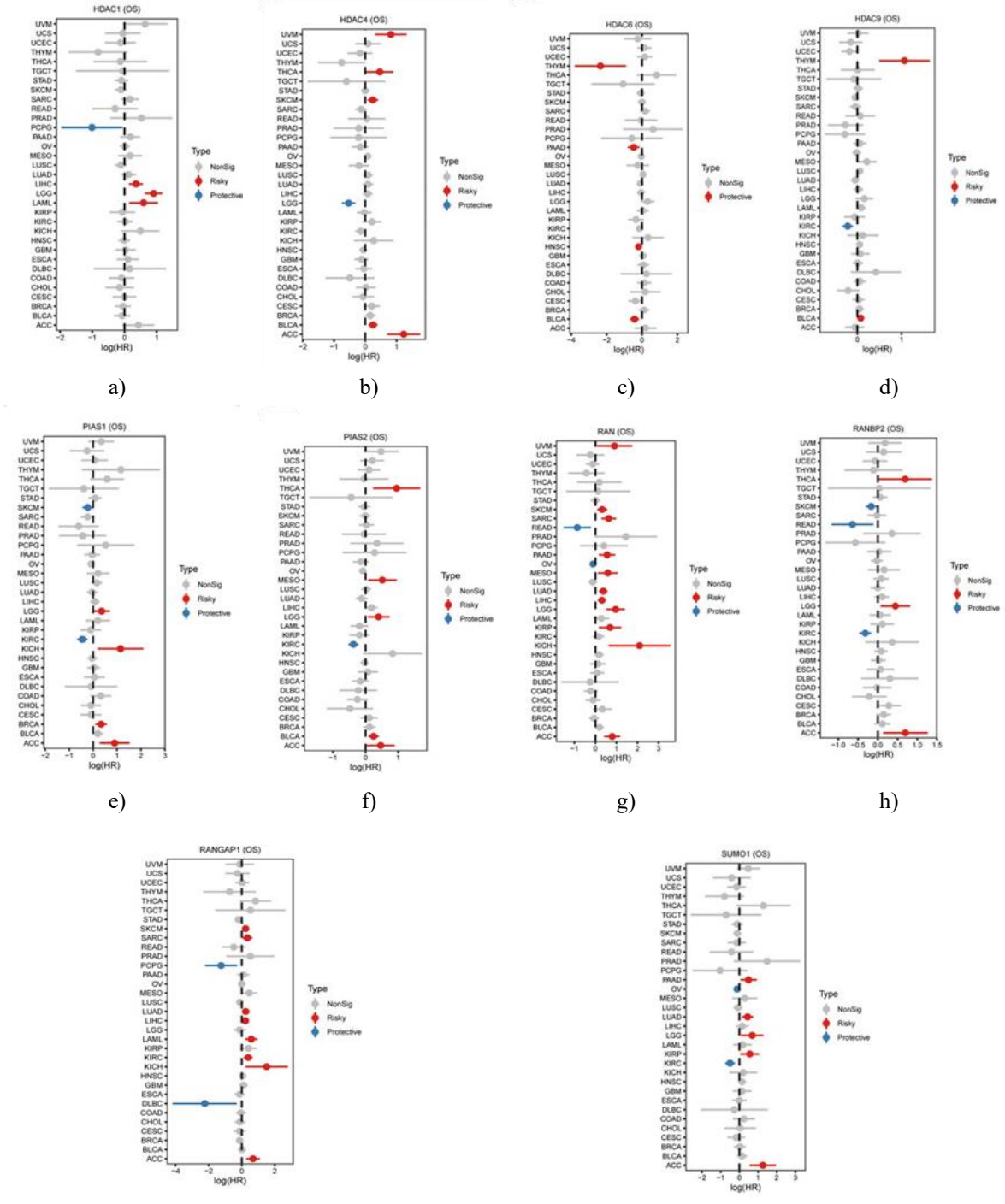

Figure 1. Association between SUMOylation-Related Gene Expression and Tumor Prognosis. (a) Forest plot illustrating hazard ratios (HRs) and 95% confidence intervals (CIs) for HDAC1 expression across multiple cancer types, indicating its impact on overall survival (OS); red denotes increased risk, whereas blue represents a protective effect. (b) Similar analysis for HDAC4, showing its influence on OS in different malignancies through corresponding HR and CI values. (c) Depiction of HDAC6 expression effects on OS, highlighting its prognostic relevance. (d) Validation of HDAC6's prognostic role using an independent dataset to confirm the observed associations. (e) HR and CI values for PIAS1, demonstrating its potential role in tumor progression and patient outcomes. (f) Forest plot for PIAS2, reflecting its prognostic significance across various cancers. (g) Association of RAN expression with OS, indicating its potential impact on survival. (h) Influence of RANBP2 expression on patient prognosis, with HR and CI values highlighting its predictive relevance. (i) Analysis of RANGAP1 expression in relation to OS, suggesting a survival-

promoting role in certain contexts. (j) HR and CI values for SUMO1, illustrating its dual role as a risk or protective factor depending on cancer type.

Relationship between SUMOylation-related gene expression and tumor prognosis

We investigated expression patterns and promoter methylation of SUMOylation-associated genes across multiple cancer types to uncover potential epigenetic regulation and functional implications. Analyses of unpaired tumor versus normal samples **(Figure 2a)** and paired tumor-normal comparisons **(Figure 2b)** revealed both significant upregulation and downregulation of SUMOylation-related genes, indicating widespread transcriptional dysregulation. These trends were further validated using TCGA-GTEx integrated datasets **(Figure 2c)**, confirming consistent expression alterations across independent cohorts.

Promoter methylation profiling **(Figure 2d)** identified genes with marked differences between tumor and normal tissues, pointing to complex epigenetic control mechanisms. Correlation analysis between methylation levels and gene expression **(Figure 2e)** revealed both positive and negative associations, underscoring the nuanced regulatory relationships governing SUMOylation-related genes. Examination of delta methylation values **(Figure 2f)** highlighted genes with abnormal epigenetic shifts, which may serve as candidate therapeutic targets. Collectively, these findings advance our understanding of the molecular networks modulating cancer progression and emphasize SUMOylation-related genes as promising biomarkers and intervention points for future research.

a)

b)

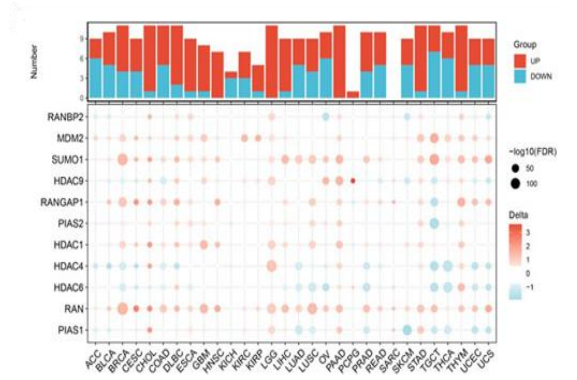

c)

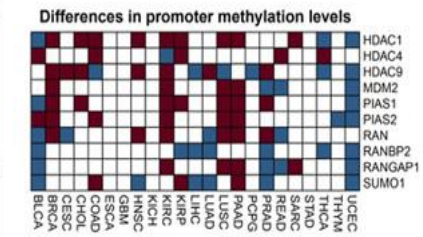

d)

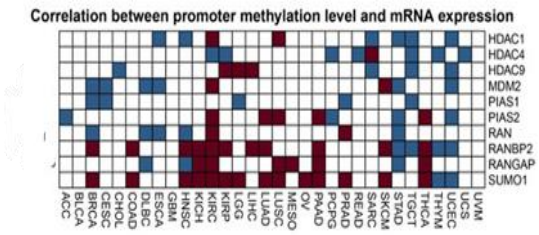

e)

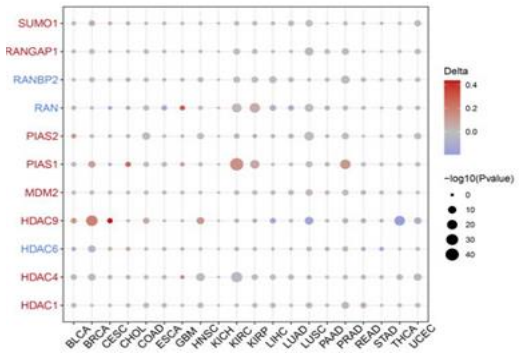

f)

Figure 2. Pan-Cancer Expression Profiles of SUMOylation-Related Genes. (a) Differential expression of SUMOylation-associated genes was evaluated across unpaired tumor and normal samples from multiple cancer types. Each row represents an individual gene, while each column corresponds to a distinct cancer. (b) Heatmap of paired tumor-normal samples illustrating expression differences of SUMOylation-related genes

within the same patients, using log2 fold-change (log2FC) values consistent with panel A. (c) Differential expression across TCGA-GTEx datasets is visualized as a dot plot, with log2FC values on the y-axis, dot size representing -log10 adjusted p-values, and colors indicating downregulation (blue) or upregulation (red). (d) Promoter methylation analysis of SUMOylation genes, where the heatmap gradient from white to dark blue reflects increasing methylation in tumor versus normal tissues. (e) Correlation between promoter methylation levels and gene expression is presented as a heatmap of Pearson correlation coefficients; dark blue represents strong negative correlations, while dark red indicates strong positive correlations. (f) Delta methylation values comparing tumor to normal tissues are illustrated in a bubble plot; bubble size corresponds to -log10 p-values, and color reflects methylation direction (red for increased, blue for decreased).

Promoter methylation analysis of SUMOylation-related genes

A detailed evaluation of promoter methylation across SUMOylation-related genes was conducted. Analysis of the HDAC1 promoter revealed variability in methylated versus unmethylated sites, with pie and circular plots highlighting regions of high methylation. HDAC4 promoter analysis demonstrated notable heterogeneity across datasets, visualized using bar and pie charts. The HDAC6 promoter showed methylation changes by sample type, while HDAC9 displayed distinct methylation hotspots potentially impacting regulation. For MDM2, methylation patterns varied under different conditions. PIAS1 revealed differential methylation across experimental groups, whereas PIAS2 showed more consistent patterns. The RAN promoter highlighted methylation levels and chromatin accessibility, with additional visualizations of potential regulatory effects. RANBP2 exhibited moderate methylation variability, while RANGAP1 showed notable differences across samples. Finally, SUMO1 demonstrated promoter methylation patterns potentially affecting expression, with bar charts, pie charts, and circular plots illustrating distribution and ATAC-seq peak locations across chromosomes.

Pan-cancer analysis: CNV, methylation, and tumor mutation burden of SUMOylation-related genes

A comprehensive investigation of genetic and epigenetic alterations of SUMOylation-associated genes across cancers was conducted. **Figure 3a** depicts Copy Number Variation (CNV) rates for these genes across 20 cancer types, with color-coded bars denoting each type. **Figure 3b** presents a bubble plot linking CNV to gene expression, where bubble size and color (red for positive correlation, blue for negative) indicate association strength and direction. **Figures 3c and 3d** illustrate the influence of Tumor Mutation Burden (TMB) and promoter methylation on gene expression, suggesting that CNV and hypermethylation contribute substantially to dysregulated expression in tumors**. Figure 3e** displays a heatmap of SUMOylation-related gene expression across tumor microenvironments, with rows representing genes and columns representing cancer types; color gradients indicate expression levels (pink = low, blue = high). These findings highlight the complex regulatory roles of SUMOylation genes in cancer and provide insights for potential targeted therapies.

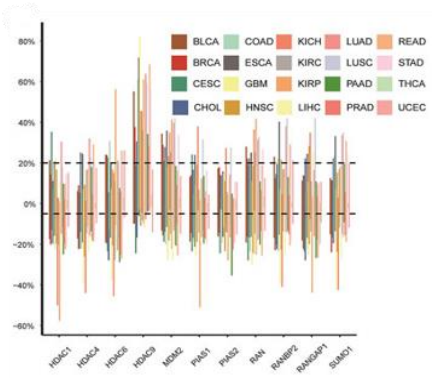

a)

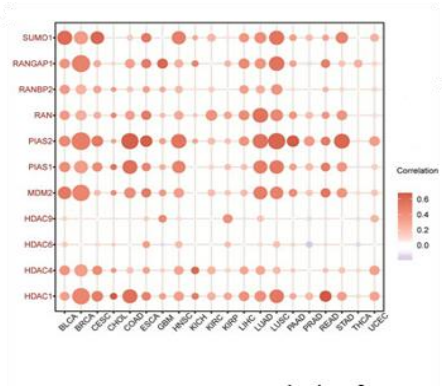

b)

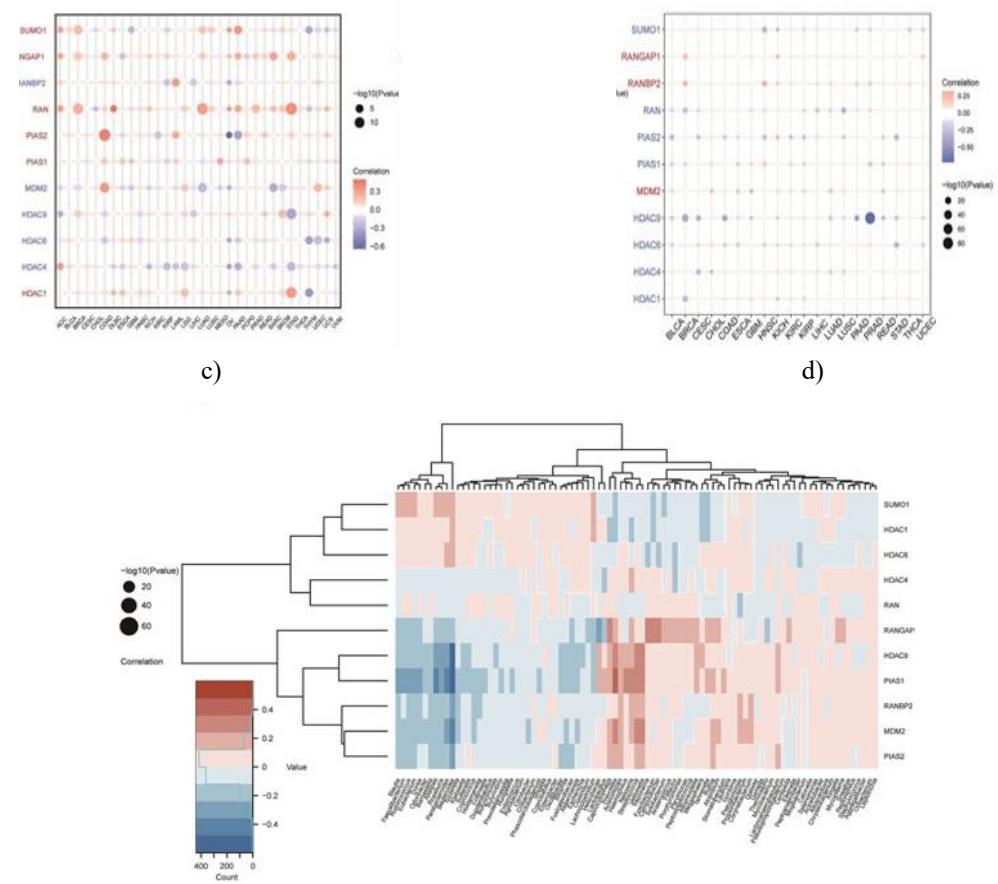

c) d)

e)

Figure 3. Pan-Cancer Analysis of SUMOylation-Related Genes: CNV, Methylation, and Tumor Mutation Burden. (a) The bar plot illustrates copy number variation (CNV) frequencies of SUMOylation-associated genes across 20 cancer types. Each bar represents a distinct cancer, color-coded according to the legend. The vertical axis indicates the percentage of samples harboring CNVs, while the horizontal axis lists the corresponding cancer types. (b) Bubble plot showing the correlation between CNV and gene expression across cancers. Bubble color indicates the correlation direction (red for positive, blue for negative), and bubble size reflects correlation magnitude. (c) Association between tumor mutation burden (TMB) and SUMOylation-related gene expression is visualized as a bubble plot; bubble size represents significance, while color intensity indicates correlation strength. (d) Correlation between promoter methylation and gene expression across cancer types is shown in a bubble plot, with bubble size denoting significance and color representing correlation direction. (e) Heatmap of SUMOylation-related gene expression across diverse tumor microenvironments. Rows correspond to genes, columns to cancer types, and the color gradient from pink to blue indicates expression levels (low to high).

Molecular docking and pathway enrichment analysis in LGG and GBM

To identify key proteins linked to low-grade glioma (LGG) prognosis, we focused on HDAC1, PIAS1, PIAS2, RAN, and RANBP2, which were found to be significant markers of poor outcome. Three-dimensional structures of these proteins were retrieved from the PDB database, and 321 small-molecule ligands from the NCBI PubChem database were screened using molecular docking. Results demonstrated that Dfo, Paromomycin, and 5-Methyltetrahydrofolate exhibited strong binding affinities with HDAC1, PIAS1, PIAS2, RAN, and RANBP2, suggesting their potential as therapeutic candidates targeting ubiquitin-like modification pathways in LGG **(Figure 4b).**

Gene Set Enrichment Analysis (GSEA) was applied to multiple cancer types to identify pathways critical for tumor progression **(Figure 4b)**. The dot plot presents normalized enrichment scores (NES), with dot size reflecting enrichment significance. Pathways including xenobiotic metabolism, epithelial-mesenchymal transition (EMT), and fatty acid metabolism were notably upregulated in cancer samples. Further, GSEA focused on SUMOylation-related gene sets in glioblastoma (GBM) revealed enrichment of these genes in tumor versus control samples

(Figure 4c). The enrichment score curve ranks genes by expression, with the histogram indicating their positions within the gene set. These analyses underscore the prominent role of SUMOylation in GBM tumorigenesis and highlight potential molecular targets for therapeutic intervention.

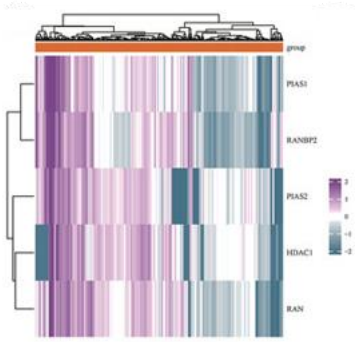

a)

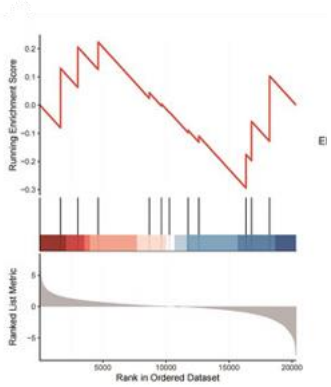

c)

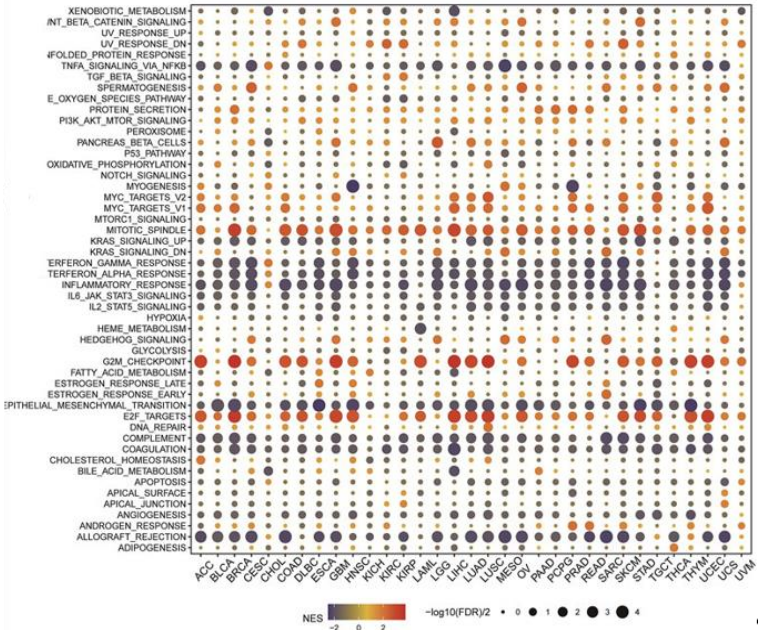

b)

Figure 4. Molecular docking and pathway enrichment analyses in Low-Grade Glioma (LGG) and Glioblastoma (GBM). (a) Core protein drug sensitivity and molecular docking heatmap: This heatmap illustrates the association between key proteins—HDAC1, PIAS1, PIAS2, RAN, and RANBP2—and patient prognosis in LGG, as identified through a pan-cancer analysis. These proteins were recognized as significant indicators of poor prognosis in LGG. To identify potential therapeutic compounds targeting these proteins, molecular docking simulations were conducted. Three-dimensional structures of the target proteins were obtained from the PDB database, and a set of 321 small-molecule ligands from the NCBI PubChem database were screened. Molecular docking was performed to evaluate ligand-protein binding affinities, quantified using LibDockScore. Results indicated that Dfo, Paromomycin, and 5-Methyltetrahydrofolate exhibited strong binding to HDAC1, PIAS1, PIAS2, RAN, and RANBP2, suggesting their potential as therapeutic candidates targeting ubiquitin-like modification pathways in LGG. (b) Pan-cancer GSEA enrichment analysis: The dot plot presents the results of gene set enrichment analysis (GSEA) across multiple cancer types. Normalized enrichment scores (NES) are indicated by color, with red representing enrichment in cancer samples and blue indicating enrichment in control samples. Dot sizes correspond to the significance of enrichment (-log10 FDR q-value). Key processes enriched in cancer include xenobiotic metabolism, epithelial-mesenchymal transition, and fatty acid metabolism. (c) GSEA of sumoylation-related gene sets in GBM: Enrichment analysis of sumoylation-associated genes in GBM compared to normal tissues was performed using the clusterProfiler package. The enrichment score curve depicts gene ranking based on expression levels, while the bar plot underneath shows gene positions in the ranked list, highlighting the extent of sumoylation-related activity enrichment in GBM.

Prognostic evaluation of SUMOylation-related genes in GBM using ssGSEA: The prognostic value of SUMOylation-related genes in GBM was assessed via single-sample GSEA (ssGSEA). Kaplan-Meier survival analyses were performed for Overall Survival (OS), Progression-Free Interval (PFI), and Disease-Specific Survival (DSS), stratified by high versus low ssGSEA scores. Higher ssGSEA scores were associated with worse

OS (**Figure 5a)**, (p = 0.022), shorter PFI **(Figure 5b)**, (p < 0.001), and decreased DSS **(Figure 5c)**, (p = 0.038). Further evaluation of OS confirmed these trends **(Figure 5d)**, (p = 0.015). A combined analysis of multiple GBM datasets (CGGA301, CGGA325, CGGA693, Rembrandt, and TCGA) using univariate Cox regression revealed that elevated ssGSEA scores correlated with poorer survival outcomes, with a pooled hazard ratio (HR) of 0.71 (95% CI: 0.47–1.06). No substantial heterogeneity was observed across datasets **(Figure 5e)**. Additional analyses of individual SUMOylation-related genes reinforced their prognostic relevance for OS **(Figure 5f),** PFI (**Figure 5g)**, and DSS **(Figure 5h)**. Collectively, these findings indicate that higher ssGSEA scores of SUMOylation-related genes are linked to unfavorable prognosis in GBM, supporting their utility as potential prognostic biomarkers.

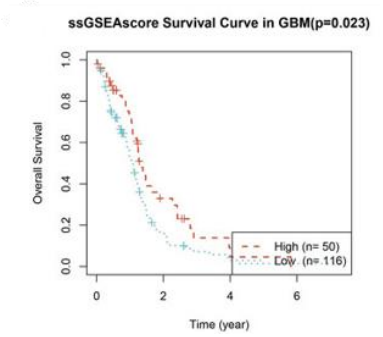

c)

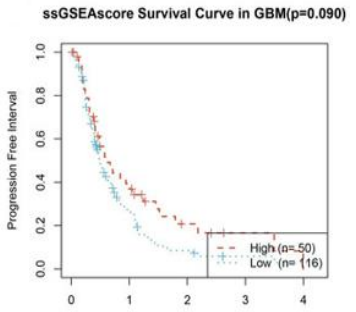

b)

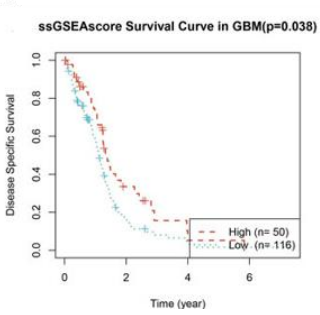

c)

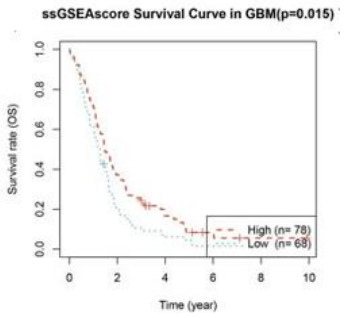

d)

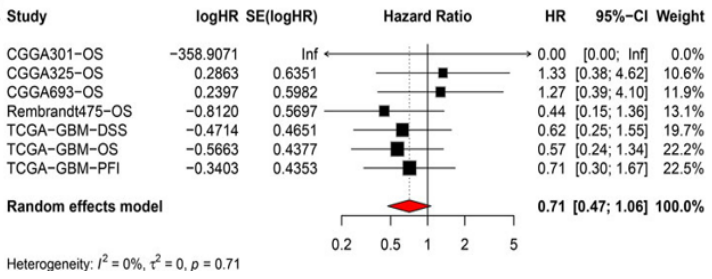

e)

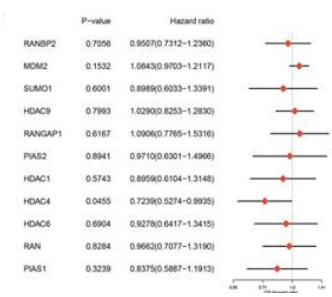

f)

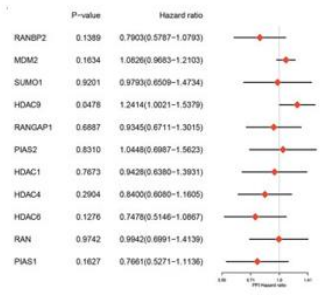

g)

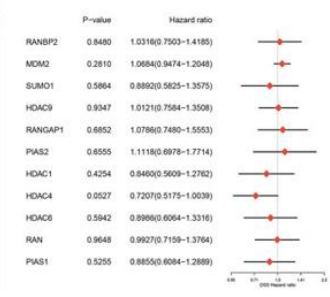

h)

Figure 5. Prognostic evaluation of SUMOylation-related genes in glioblastoma (GBM) using ssGSEA. (a–d) Kaplan-Meier survival analyses: Single-sample gene set enrichment analysis (ssGSEA) scores for SUMOylation-related genes were used to stratify GBM patients into high- and low-score groups. Survival

outcomes assessed included Overall Survival (OS, a), Progression-Free Interval (PFI, b), and Disease-Specific Survival (DSS, c). Statistically significant differences between groups are indicated by p-values. Publicly available GBM datasets were used for this analysis. (e) Meta-analysis of univariate Cox regression for OS: A combined analysis of multiple GBM cohorts (CGGA301, CGGA325, CGGA693, Rembrandt, and TCGA) was performed. The forest plot presents log hazard ratios (logHR), standard errors (SE), hazard ratios (HR), 95% confidence intervals (CI), and study weights. A random-effects model calculated the pooled HR while accounting for heterogeneity among datasets. (f–h) Hazard ratios of individual SUMOylation-related genes: Forest plots depict the prognostic significance of individual genes for OS (f), PFI (g), and DSS (h) across the various GBM datasets, including p-values, HRs, and confidence intervals. These results provide insight into the potential prognostic relevance of each SUMOylation-related gene.

Prognostic model of SUMOylation-related genes in GBM

The study aimed to construct and validate a predictive model based on the expression of SUMOylation-related genes in GBM. The observed data are represented by the red line, while the dashed blue line indicates perfect prediction. The Hosmer-Lemeshow test confirmed good agreement between observed and predicted probabilities. ROC curve analysis suggested limited diagnostic accuracy. These results indicate that although the ssGSEA-based model is well-calibrated, its ability to discriminate tumor from normal tissues in GBM is modest, warranting further optimization to improve diagnostic utility.

Paromomycin suppresses SUMOylation-related gene activity and reduces GBM cell viability

Paromomycin treatment was found to inhibit SUMOylation-related gene expression and decrease the viability of GBM cells. As shown in **Figure 6a**, cell viability decreased in a dose-dependent manner. qRT-PCR analysis revealed significant reductions in mRNA levels of HDAC1, PIAS1, PIAS2, and RANBP2 with increasing Paromomycin concentrations **(Figures 6b–6e)**. Immunofluorescence staining demonstrated enhanced caspase-3 activity and decreased SUMO1 expression at higher Paromomycin doses **(Figures 6f and 6g)**. Additionally, colony formation assays confirmed reduced glioma cell proliferation.

In U-251MG glioblastoma cells, Paromomycin significantly reduced cell viability **(Figure 7a)**. CCK8 assays indicated a dose-dependent decrease in OD450 values, which was more pronounced when Paromomycin was combined with the HDAC1 inhibitor TSA, suggesting enhanced antiproliferative effects. Colony formation assays further validated this inhibitory effect, showing a marked reduction in colonies in the Paromomycin group, while TSA co-treatment partially restored proliferation **(Figures 7b and 7c)**.

Transwell migration assays demonstrated that Paromomycin impaired U-251MG cell migration, an effect reversed by TSA co-treatment **(Figure 7d)**. Immunofluorescence analyses revealed that Paromomycin reduced IGF1R nuclear translocation, potentially by altering SUMO1 modification, with TSA reversing this effect **(Figure 7e)**.

Overall, these results indicate that Paromomycin not only suppresses GBM cell survival and proliferation but also modulates key SUMOylation-related genes and pathways, suggesting its potential as a therapeutic agent for GBM **(Figure 8)**.

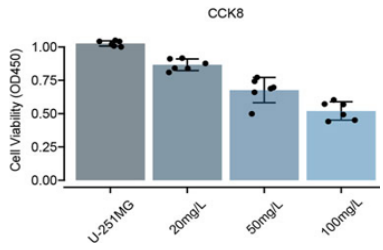

a)

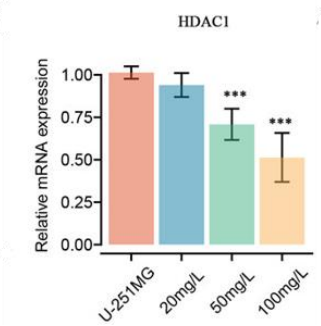

b)

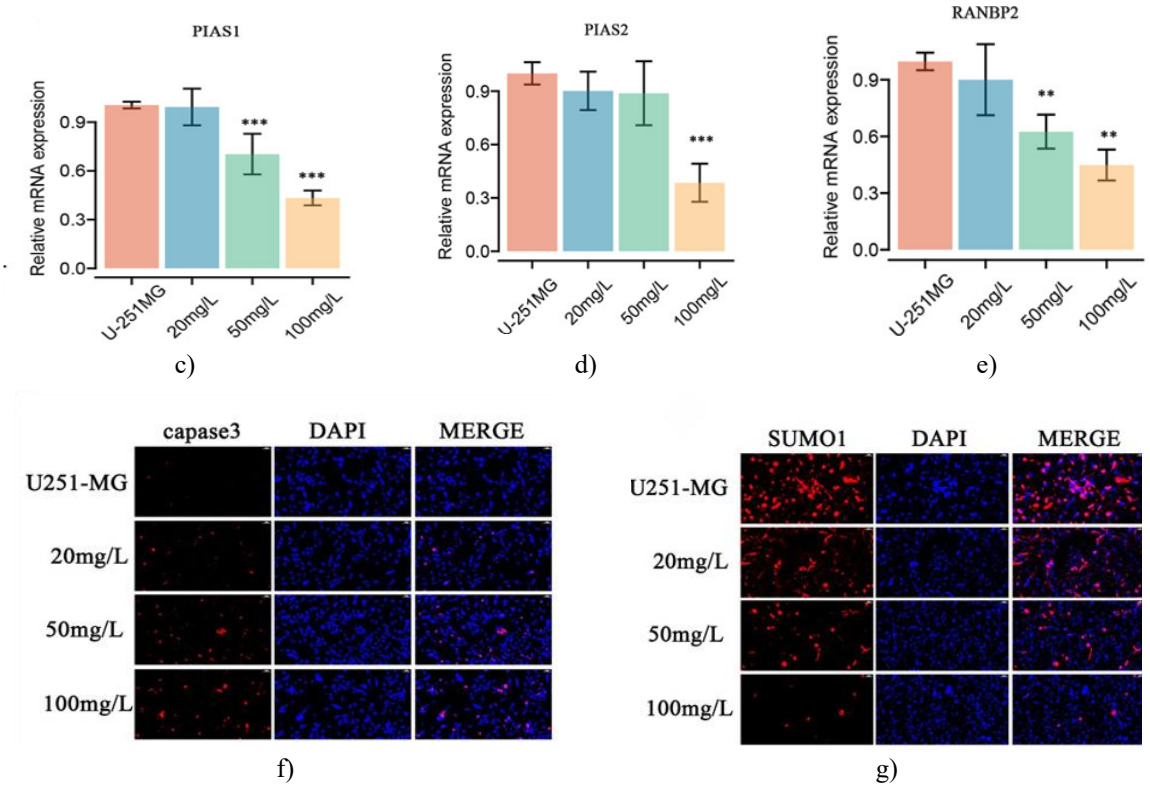

Figure 6. Impact of Paromomycin on U-251MG Glioblastoma Cell Viability, Gene Expression, Apoptosis, SUMOylation, and Colony Formation. (a) Cell viability assessment: The CCK8 assay was used to measure U-251MG cell proliferation following treatment with different concentrations of Paromomycin (20, 50, and 100 mg/L). A dose-dependent decrease in optical density (OD450) was observed, indicating that Paromomycin effectively suppresses cell growth. b–e) qRT-PCR analysis of SUMOylation-related genes: Relative mRNA levels of HDAC1, PIAS1, PIAS2, and RANBP2 were measured after Paromomycin treatment at varying doses. The results demonstrated significant, dose-dependent downregulation of these genes, with the strongest suppression at 100 mg/L. Statistical significance is indicated as **p < 0.01 and ***p < 0.001 compared to untreated controls. (f) Apoptosis evaluation: Immunofluorescence staining for caspase-3 (red), an apoptosis marker, revealed increased expression in cells treated with escalating doses of Paromomycin, suggesting induction of apoptosis. (g) Assessment of SUMOylation: Immunofluorescence for SUMO1 (red), with nuclei counterstained using DAPI (blue), showed a marked reduction in SUMO1 levels across all Paromomycin concentrations, indicating inhibition of protein SUMOylation.

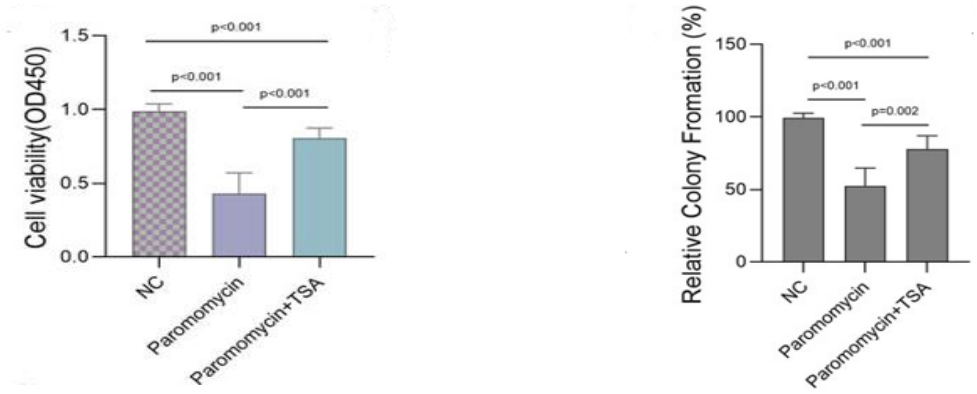

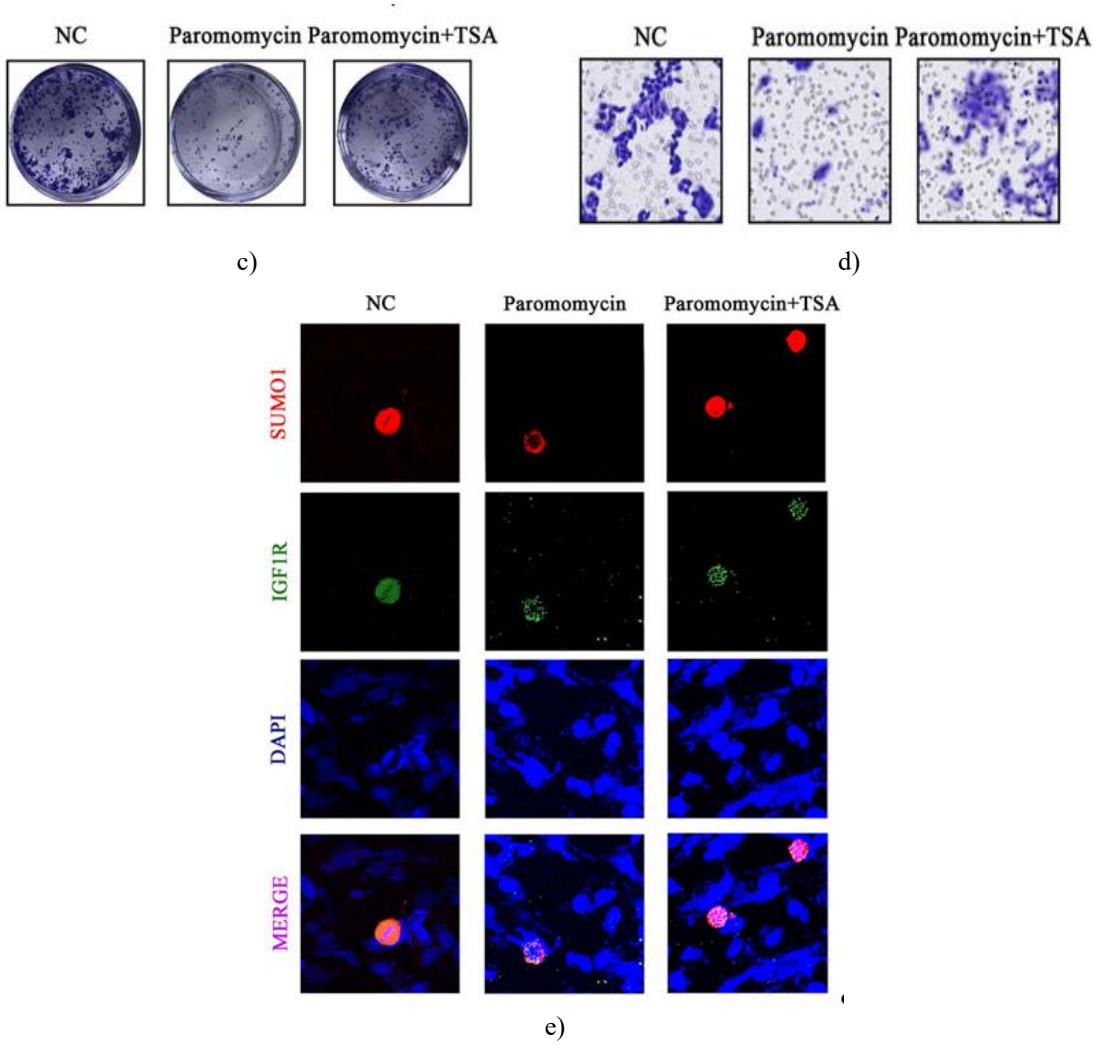

Figure 7. Paromomycin's effects on proliferation, colony formation, migration, and SUMOylation in U-251MG glioblastoma cells. (a) Proliferation assay: U-251MG cells were exposed to Paromomycin alone or combined with TSA, and cell growth was measured via CCK8. Results indicate that Paromomycin markedly reduced cell proliferation relative to the negative control, with a further decrease observed when co-administered with TSA (*$p < 0.001$). (b) Colony formation quantification: The relative percentage of colony formation was calculated, showing that both Paromomycin alone and its combination with TSA substantially diminished colony numbers compared with the control group (*$p < 0.001$, **$p = 0.002$). (c) Representative colony images: Microscopic examination demonstrates that Paromomycin reduces colony size and density, and the effect is amplified with TSA co-treatment. (d) Cell migration assessment: Transwell assays reveal that Paromomycin restricts U-251MG cell migration. Cells treated with Paromomycin displayed fewer migrating cells, and co-treatment with TSA modified this effect. (e) SUMO1 and IGF1R localization: Immunofluorescence staining was performed for SUMO1 (red) and IGF1R (green), with nuclei counterstained with DAPI (blue). Paromomycin decreased IGF1R nuclear translocation, suggesting a potential link between its effect on IGF1R trafficking and SUMO1 modification.

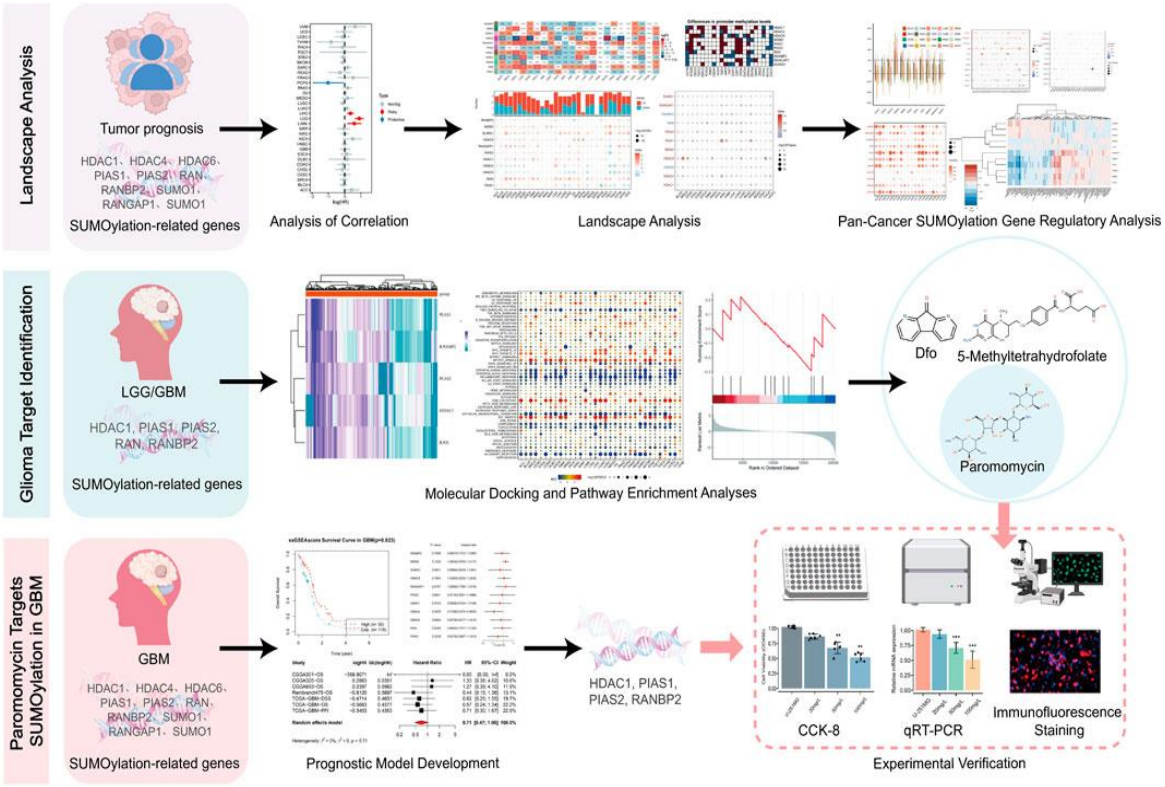

Figure 8. Combined bioinformatics and experimental investigation of Paromomycin targeting HDAC1 in GBM.

Results and Discussion

Glioblastoma (GBM) is an extremely aggressive brain malignancy characterized by poor survival outcomes and a high likelihood of recurrence. Despite advances in research and clinical management, the five-year survival rate for GBM patients remains below 5%, underscoring the urgent need for novel therapeutic approaches [38, 65]. Our results indicate that Paromomycin, an aminoglycoside antibiotic, can effectively target HDAC1, thereby inhibiting GBM progression. Recent technological and molecular advances have greatly enhanced disease understanding, facilitating the development of targeted therapeutic strategies [66-68].

Extensive studies of gene expression and regulatory mechanisms within biological systems have yielded crucial insights into gene function and regulation [69-71]. Protein-protein interaction networks and their regulatory variations are increasingly recognized as central to cell signaling and functional control, highlighting their importance in disease biology [72-74]. Such research not only deepens our understanding of pathophysiology but also provides a solid foundation for experimental and clinical treatment strategies [17, 75-79].

The integration of bioinformatics and large-scale datasets is becoming increasingly critical for identifying biomarkers, improving disease diagnosis, and predicting clinical outcomes [80-83]. Insights into cell death pathways, metabolic regulation, and cytokine signaling have expanded potential therapeutic targets and informed drug development [84-88]. Additionally, studies examining exercise-mediated regulation of monocyte gene expression in Alzheimer's disease have suggested novel therapeutic avenues [89-91].

Our analysis revealed that high HDAC1 expression is associated with poor prognosis across multiple cancer types, indicating its potential utility as both a prognostic biomarker and a therapeutic target. Using a combination of bioinformatics and experimental validation, we show that Paromomycin can selectively inhibit HDAC1 to suppress GBM cell growth. Evaluation of SUMOylation-related genes across various cancers highlighted distinct expression patterns and methylation differences, supporting the relevance of epigenetic regulation in malignancy.

HDAC1 is a pivotal histone deacetylase that regulates chromatin structure and gene expression by removing acetyl groups from histones [92]. It plays essential roles in controlling cell cycle progression, differentiation, and apoptosis [93]. Dysregulated HDAC1 contributes to the development and aggressiveness of cancers, including GBM, by promoting cell proliferation, migration, and resistance to apoptosis. Overexpression of HDAC1 suppresses tumor suppressor genes and activates oncogenic pathways, enhancing tumor survival. Its role in

maintaining the self-renewal capacity of GBM stem cells further complicates treatment, as these cells are resistant to standard therapies [94].

Our study demonstrates that Paromomycin inhibits HDAC1, counteracting harmful epigenetic modifications that drive GBM progression. By targeting HDAC1, Paromomycin may reactivate genes that limit proliferation or promote apoptosis, potentially enhancing the effectiveness of conventional therapeutic regimens.

The pursuit of targeted therapies has become central to improving clinical outcomes while reducing side effects, driving advances in precision medicine [95-97]. Among potential candidates, Paromomycin—a well-known aminoglycoside antibiotic—has rarely been explored for anticancer activity [98]. Through in silico molecular docking of FDA-approved compounds, Paromomycin emerged as a promising inhibitor of HDAC1, demonstrating strong binding interactions that suggest its capacity to modulate both HDAC1 activity and the SUMOylation pathway. This mechanism presents a novel opportunity to specifically target SUMOylation in glioblastoma (GBM) and potentially develop new therapeutic approaches.

Our study indicates that Paromomycin may effectively suppress GBM growth by interfering with HDAC1 and regulating IGF1R SUMOylation, offering a strategy that could also be extended to other cancers [99]. HDAC1 (histone deacetylase 1) is a key epigenetic regulator that alters chromatin structure via deacetylation, often promoting oncogenic gene expression across multiple tumor types [100]. In GBM, aberrant HDAC1 function is linked to enhanced proliferation, invasiveness, and poor clinical outcomes. Therefore, inhibiting HDAC1 with Paromomycin may disrupt critical HDAC1-driven signaling, reducing tumor cell proliferation and aggressiveness. Experimental validation supports this mechanism. Paromomycin specifically targets SUMOylated HDAC1 in GBM cells, significantly reducing proliferation, motility, and invasiveness [45, 101, 102]. In U-251MG cells, CCK-8 assays demonstrated a clear dose-dependent reduction in viability, confirming the drug's antiproliferative effect. qRT-PCR analyses further revealed decreased expression of HDAC1 and other SUMOylation-related genes, including PIAS1, PIAS2, and RANBP2. Immunofluorescence staining showed elevated caspase-3 levels alongside reduced SUMO1 expression, indicating activation of apoptosis and suppression of protein SUMOylation.

Beyond GBM, advances in targeted therapy have enhanced treatment efficacy, reduced toxicity, and promoted precision medicine initiatives [95]. Systematic reviews and meta-analyses have contributed substantially to biomedical research, particularly in drug discovery and bioinformatics, bridging fundamental studies with translational applications [103]. Insights into cell death mechanisms and metabolic regulation have further identified promising therapeutic targets [104], while selective inhibition of proteins or signaling pathways has improved treatment specificity and potency [105]. For example, kiwi root extract has shown efficacy against gastric cancer [106], and integrating contemporary technology with traditional Chinese medicine provides innovative perspectives in drug development [107]. Recent advances in materials science have enabled the creation of novel composites with broad applications in biomedical engineering [108].

Traditionally, Paromomycin has been used to treat intestinal infections and amebiasis [109]. Its emerging role in cancer therapy highlights its potential to inhibit HDAC1, altering tumor cell epigenetics and reducing proliferation and invasiveness. Nuclear IGF1R, a key regulator of proliferation and survival, appears influenced by Paromomycin via SUMOylation modulation, further contributing to its antitumor effect. Given its established pharmacological profile, safety, and clinical usage, repurposing Paromomycin as an HDAC1-targeted agent offers a cost-effective strategy for GBM treatment, with broader implications for other malignancies.

In both tumors and neurological disorders, SUMOylation plays a pivotal role in regulating key cellular processes such as proliferation, differentiation, and apoptosis by modulating the function of specific proteins and receptors [110]. Among these, IGF1R, a transmembrane receptor tyrosine kinase, is critical for cell growth, differentiation, survival, and metabolic regulation [111] Beyond its general cellular functions, IGF1R is essential for nervous system development, neuronal survival, and synaptic plasticity, linking its functional regulation closely to the progression of multiple diseases [112]. SUMOylation of IGF1R has been shown to influence downstream signaling efficiency, thereby potentially restraining tumor cell proliferation and migration [113]. Therapeutically, targeting IGF1R SUMOylation could provide a distinct advantage over conventional IGF1R inhibitors by minimizing off-target effects while enhancing efficacy [113, 114]

HDAC1 contributes not only to acetylation dynamics but also interacts with other post-translational modifications, including SUMOylation. The activity of HDAC1 may affect the expression or function of SUMO-related enzymes, thereby modulating the SUMOylation status of proteins such as IGF1R. Consequently, HDAC1 inhibitors, including Paromomycin, could influence IGF1R signaling in tumors through changes in its

SUMOylation, providing insight into the interplay between HDAC1 activity and SUMOylation in tumor progression. Targeting HDAC1 to control IGF1R SUMOylation represents a promising strategy in cancer research, offering potential therapeutic opportunities and addressing drug resistance. Our data indicate that HDAC1 activity may regulate IGF1R nuclear translocation, with inhibition of HDAC1 potentially reducing IGF1R SUMO1 modification, thereby altering its nuclear localization and downstream signaling.

Although our analysis did not reveal a significant correlation between HDAC1 expression and overall survival in GBM, nor pronounced differences in methylation levels, this does not negate SUMOylation's role in tumor biology. SUMOylation is a complex post-translational modification influencing tumor growth through diverse mechanisms. The absence of a strong association between HDAC1 or other SUMO-related genes and GBM in our dataset may reflect context-dependent or indirect effects, rather than the lack of functional relevance. For example, HDAC1-mediated regulation of IGF1R SUMOylation could affect cellular proliferation and invasiveness under specific conditions, yet these effects may be obscured in heterogeneous clinical datasets. Given that SUMOylation involves multiple proteins and genes, its impact may vary across tumor types or stages. Even when statistical significance is limited, unexamined SUMO-related genes or specific subgroups may still play critical roles. SUMOylation can influence both tumor-suppressive and oncogenic proteins, such as enhancing MDM2 activity, which promotes proliferation and survival [115], particularly in gliomas and other cancers. It also plays a central role in nuclear translocation of proteins [114, 116], underscoring the need for further investigation into individual SUMO-related genes and subtype-specific effects.

Exercise has been shown to affect nuclear translocation across numerous signaling pathways, including those regulating metabolism and cellular repair [117]. Physical activity can slow tumor progression by modulating immune responses, reducing pro-inflammatory factors, and improving metabolic homeostasis. The exercise-induced regulation of nuclear translocation is crucial for cell adaptation, repair, and antioxidant responses. If Paromomycin modulates nuclear translocation pathways through HDAC1, it could potentiate the beneficial effects of exercise, particularly in elderly or chronically ill individuals where adaptive metabolic responses are limited. As an HDAC1 inhibitor, Paromomycin may influence gene expression, metabolic regulation, and anti-tumor mechanisms linked to exercise, although further experimental validation is required.

Overall, precision medicine approaches, including targeted therapies and immunotherapies, are being actively explored to enhance patient outcomes and quality of life [36, 118]. Integration of multi-omics, bioinformatics, and machine learning approaches—such as small molecule screening, deep learning, and pathway analysis—offers new avenues for personalized treatment strategies [96, 119-121]. Clinical decision-making tools, including shared decision-making frameworks and checklists, are recommended to optimize therapy selection and patient engagement [29, 31]. Improvements in drug delivery systems and nanotechnology could further enhance therapeutic targeting and efficacy. Combining Paromomycin with other treatment modalities may strengthen its therapeutic impact, providing a comprehensive strategy against GBM. These findings provide a foundation for future drug development and translational research to bring HDAC1- and SUMOylation-targeted therapies to clinical application [95, 122-125]. Further studies are warranted to elucidate the precise molecular mechanisms of Paromomycin in modulating HDAC1 and the SUMOylation pathway, including gene expression and methylation analyses in human GBM samples, to ensure clinical relevance.

Conclusion

This research underscores the pivotal influence of SUMOylation-associated genes on cancer outcomes. Paromomycin demonstrates therapeutic potential in glioblastoma (GBM) by inhibiting cell proliferation and migration, as well as modulating SUMO1 modification and IGF1R nuclear translocation. These results indicate that interfering with SUMOylation pathways using Paromomycin could represent a promising approach for GBM therapy, opening avenues for the development of novel targeted cancer treatments.

Acknowledgments: The authors declare that the use of GPT-4.0 for academic editing purposes only, which contributed to language refinement and clarity in presenting the study's findings. All intellectual and scientific content is solely the result of the authors' original research and analysis.

Conflict of Interest: None

Financial Support: The author(s) declare that financial support was received for the research, authorship, and/or publication of this article. This project was funded by the Special Task Grant for the Construction of an Innovative Province in Hunan (Project No. 2424JJ7043).

Ethics Statement: None.

References

1. Banu Z. Glioblastoma multiforme: a review of its pathogenesis and treatment. Int Res J Pharm. 2019;9:7-12.
2. Grochans S, Cybulska AM, Simińska D, Korbecki J, Kojder K, Chlubek D, et al. Epidemiology of glioblastoma multiforme–literature review. Cancers (Basel). 2022;14(10):2412.
3. Yalamarty SSK, Filipczak N, Li X, Subhan MA, Parveen F, Ataide JA, et al. Mechanisms of resistance and current treatment options for glioblastoma multiforme (GBM). Cancers (Basel). 2023;15(7):2116.
4. Tian Y, Zhou Y, Chen F, Qian S, Hu X, Zhang B, et al. Research progress in MCM family: focus on the tumor treatment resistance. Biomed Pharmacother. 2024;173:116408.
5. Davis M. Glioblastoma: overview of disease and treatment. Clin J Oncol Nurs. 2016;20(5 Suppl):S2-8.
6. Stylli SS. Novel treatment strategies for glioblastoma—a summary. Cancers (Basel). 2021;13(22):5868.
7. Grech N, Dalli T, Mizzi S, Meilak L, Calleja N, Zrinzo A. Rising incidence of glioblastoma multiforme in a well-defined population. Cureus. 2020;12(5):e8195.
8. Ostrom QT, Kinnersley B, Armstrong G, Rice T, Chen Y, Wiencke JK, et al. Age-specific genome-wide association study in glioblastoma identifies increased proportion of 'lower grade glioma'-like features associated with younger age. Int J Cancer. 2018;143(10):2359-66.
9. Tosakoon S, Lawrence WR, Shiels MS, Jackson SS. Sex differences in cancer incidence rates by race and ethnicity: results from the surveillance, epidemiology, and end results (SEER) Registry (2000-2019). J Clin Oncol. 2023;41(16_suppl):10547.
10. Dasari A, Saini M, Sharma S, Bergemann R. Pro15 healthcare resource utilisation and economic burden of glioblastoma in the United States: a systematic review. Value Health. 2020;23:S331.
11. Aly A, Singh P, Korytowsky B, Ling YL, Kale HP, Dastani HB, et al. Survival, costs, and health care resource use by line of therapy in US Medicare patients with newly diagnosed glioblastoma: a retrospective observational study. Neurooncol Pract. 2020;7(2):164-75.
12. Elsaid MI, John T, Li Y, Pentakota SR, Rustgi VK. The health care burden of hepatic encephalopathy. Clin Liver Dis. 2020;24(2):263-75.
13. Nakada M, Kita D, Watanabe T, Hayashi Y, Teng L, Pyko IV, et al. Aberrant signaling pathways in glioma. Cancers (Basel). 2011;3(3):3242-78.
14. Kesari S. Understanding glioblastoma tumor biology: the potential to improve current diagnosis and treatments. Semin Oncol. 2011;38 Suppl 4:S2-10.
15. Nguyen HM, Guz-Montgomery K, Lowe DB, Saha D. Pathogenetic features and current management of glioblastoma. Cancers (Basel). 2021;13(4):856.
16. Chen HM, Nikolic A, Singhal D, Gallo M. Roles of chromatin remodelling and molecular heterogeneity in therapy resistance in glioblastoma. Cancers (Basel). 2022;14(19):4942.
17. Du Y, Liu H. Exercise-induced modulation of miR-149-5p and MMP9 in LPS-triggered diabetic myoblast ER stress: licorice glycoside E as a potential therapeutic target. Tradit Med Res. 2024;9:45.
18. McNerney MP, Styczynski MP. Small molecule signaling, regulation, and potential applications in cellular therapeutics. Wiley Interdiscip Rev Mech Dis. 2018;10(2):e1405.
19. Cheng Y, Ren X, Hait WN, Yang JM. Therapeutic targeting of autophagy in disease: biology and pharmacology. Pharmacol Rev. 2013;65(4):1162-97.
20. Liao Z, Lin H, Liu S, Krafft PR. Admission triglyceride-glucose index predicts long-term mortality patients with subarachnoid hemorrhage a retrospective analysis of the MIMIC-IV database. Brain Hemorrhages. 2023;5:29-37.
21. Tsuji M, Ishida F, Sato T, Furukawa K, Miura Y, Yasuda R, et al. Computational fluid dynamics using dual-layer porous media modeling to evaluate the hemodynamics of cerebral aneurysm treated with FRED: a technical note. Brain Hemorrhages. 2023;4:39-43.

22. Wu WT, Li YJ, Feng AZ, Li L, Huang T, Xu AD, et al. Data mining in clinical big data: the frequently used databases, steps, and methodological models. Mil Med Res. 2021;8(1):44.
23. Asano Y. How to eliminate uncertainty in clinical medicine – clues from creation of mathematical models followed by scientific data mining. EBioMedicine. 2018;34:12-3.
24. Srivastava V, Kumar A. Bioinformatics tools: essential for the development and discovery of medicines. TURCOMAT. 2024;11:11.
25. Li L. The potential of translational bioinformatics approaches for pharmacology research. Br J Clin Pharmacol. 2015;80(5):862-7.
26. Behl T, Kaur I, Sehgal A, Singh S, Bhatia S, Al-Harrasi A, et al. Bioinformatics accelerates the major tetrad: a real boost for the pharmaceutical industry. Int J Mol Sci. 2021;22(12):6184.
27. Pechanova O. Why we still need reliable animal models. Pathophysiology. 2020;27(1):44-5.
28. McGonigle P, Ruggeri B. Animal models of human disease: challenges in enabling translation. Biochem Pharmacol. 2014;87(1):162-71.
29. Li S, Xie J, Chen Z, Yan J, Zhao Y, Cong Y, et al. Key elements and checklist of shared decision-making conversation on life-sustaining treatment in emergency: a multispecialty study from China. World J Emerg Med. 2023;14(5):380-5.
30. Wieringa TH, Rodriguez-Gutierrez R, Spencer-Bonilla G, de Wit M, Ponce OJ, Sanchez-Herrera MF, et al. Decision aids that facilitate elements of shared decision making in chronic illnesses: a systematic review. Syst Rev. 2019;8(1):121.
31. Shan Y, Zhao Y, Li C, Gao J, Song G, Li T. Efficacy of partial and complete resuscitative endovascular balloon occlusion of the aorta in the hemorrhagic shock model of liver injury. World J Emerg Med. 2024;15(1):10-5.
32. Hao Y, Liu Z, Riter RN, Kalantari S. Advancing patient-centered shared decision-making with AI systems for older adult cancer patients. In: Proceedings of the CHI conference on human factors in computing systems. Honolulu HI, USA: ACM; 2024. p. 1-20.
33. Wang JH, Wang KH, Chen YH. Overlapping group screening for detection of gene-environment interactions with application to TCGA high-dimensional survival genomic data. BMC Bioinformatics. 2022;23(1):202.
34. Kumar HR, Zhong X, Sandoval JA, Hickey RJ, Malkas LH. Applications of emerging molecular technologies in glioblastoma multiforme. Expert Rev Neurother. 2008;8(10):1497-506.
35. Kaynar A, Altay O, Li X, Zhang C, Turkez H, Uhlén M, et al. Systems biology approaches to decipher the underlying molecular mechanisms of glioblastoma multiforme. Int J Mol Sci. 2021;22(24):13213.
36. Yang H, Cai J. Top ten breakthroughs in clinical hypertension research in 2022. CVIA. 2023;8:8.
37. Wayteck L, Breckpot K, Demeester J, De Smedt SC, Raemdonck K. A personalized view on cancer immunotherapy. Cancer Lett. 2014;352(1):113-25.
38. Aldoghachi AF, Aldoghachi AF, Breyne K, Ling KH, Cheah PS. Recent advances in the therapeutic strategies of glioblastoma multiforme. Neuroscience. 2022;491:240-70.
39. Kim HJ, Kim DY. Present and future of anti-glioblastoma therapies: a deep look into molecular dependencies/features. Molecules. 2020;25(20):4641.
40. Ou A, Yung WKA, Majd N. Molecular mechanisms of treatment resistance in glioblastoma. Int J Mol Sci. 2020;22(1):351.
41. Wu W, Klockow JL, Zhang M, Lafortune F, Chang E, Jin L, et al. Glioblastoma multiforme (GBM): an overview of current therapies and mechanisms of resistance. Pharmacol Res. 2021;171:105780.
42. Woo CH, Abe J. SUMO—a post-translational modification with therapeutic potential? Curr Opin Pharmacol. 2010;10(2):146-55.
43. Zhao H, Ding R, Han J. SUMOylation as a therapeutic target for myocardial infarction. Front Cardiovasc Med. 2021;8:701583.
44. Han ZJ, Feng YH, Gu BH, Li YM, Chen H. The post-translational modification, SUMOylation, and cancer (Review). Int J Oncol. 2018;52(4):1081-94.
45. Fox BM, Janssen A, Estevez-Ordonez D, Gessler F, Vicario N, Chagoya G, et al. SUMOylation in glioblastoma: a novel therapeutic target. Int J Mol Sci. 2019;20(8):1853.
46. Backes C, Harz C, Fischer U, Schmitt J, Ludwig N, Petersen BS, et al. New insights into the genetics of glioblastoma multiforme by familial exome sequencing. Oncotarget. 2015;6(8):5918-31.

47. Pasche B, Myers RM. One step forward toward identification of the genetic signature of glioblastomas. JAMA. 2009;302(3):325-6.
48. Lynes JP, Nwankwo AK, Sur HP, Sanchez VE, Sarpong KA, Ariyo OI, et al. Biomarkers for immunotherapy for treatment of glioblastoma. J Immunother Cancer. 2020;8(1):e000348.
49. Miller JJ, Shih HA, Andronesi OC, Cahill DP. Isocitrate dehydrogenase-mutant glioma: evolving clinical and therapeutic implications. Cancer. 2017;123(23):4535-46.
50. Yan H, Parsons DW, Jin G, McLendon R, Rasheed BA, Yuan W, et al. IDH1 and IDH2 mutations in gliomas. N Engl J Med. 2009;360(8):765-73.
51. Monti P, Menichini P, Speciale A, Cutrona G, Fais F, Taiana E, et al. Heterogeneity of TP53 mutations and P53 protein residual function in cancer: does it matter? Front Oncol. 2020;10:593383.
52. Vaddavalli PL, Schumacher B. The p53 network: cellular and systemic DNA damage responses in cancer and aging. Trends Genet. 2022;38(6):598-612.
53. Szopa W, Burley TA, Kramer-Marek G, Kaspera W. Diagnostic and therapeutic biomarkers in glioblastoma: current status and future perspectives. Biomed Res Int. 2017;2017:8013575.
54. Glass K. Using multi-omic data to model gene regulatory networks. Biotechnol Adv. 2023;49:107739.
55. Sun YV, Hu YJ. Integrative analysis of multi-omics data for discovery and functional studies of complex human diseases. Adv Genet. 2016;93:147-90.
56. Yan C, Chen Y, Sun C, Ahmed MA, Bhan C, Guo Z, et al. Does proton pump inhibitor use lead to a higher risk of coronavirus disease 2019 infection and progression to severe disease? A meta-analysis. Jpn J Infect Dis. 2022;75(1):10-5.
57. Chen Y, Cai Y, Kang X, Zhou Z, Qi X, Ying C, et al. Predicting the risk of sarcopenia in elderly patients with patellar fracture: development and assessment of a new predictive nomogram. PeerJ. 2020;8:e8793.
58. Cavill R, Jennen D, Kleinjans J, Briedé JJ. Transcriptomic and metabolomic data integration. Brief Bioinform. 2016;17(5):891-901.
59. Guo Z, Yu X, Zhao S, Zhong X, Huang D, Feng R, et al. SIRT6 deficiency in endothelial cells exacerbates oxidative stress by enhancing HIF1α accumulation and H3K9 acetylation at the Ero1α promoter. Clin Transl Med. 2023;13(7):e1377.
60. Huang L, Jiang X, Gong L, Xing D. Photoactivation of akt1/gsk3β isoform-specific signaling Axis promotes pancreatic β-cell regeneration: lpli induces β-cell replication. J Cell Biochem. 2015;116(8):1741-54.
61. Huang L, Tang Y, Xing D. Activation of nuclear estrogen receptors induced by low-power laser irradiation via PI3-K/Akt signaling cascade. J Cell Physiol. 2013;228(5):1045-59.
62. Wang F, Chen TS, Xing D, Wang JJ, Wu YX. Measuring dynamics of caspase-3 activity in living cells using FRET technique during apoptosis induced by high fluence low-power laser irradiation. Lasers Surg Med. 2005;36(1):2-7.
63. Huang L, Liu P, Yang Q, Wang Y. The KRAB domain-containing protein ZFP961 represses adipose thermogenesis and energy expenditure through interaction with PPAR α. Adv Sci (Weinh). 2022;9(11):2102949.
64. Yang X, Huang K, Yang D, Zhao W, Zhou X. Biomedical big data technologies, applications, and challenges for precision medicine: a review. Glob Chall. 2024;8(1):2300163.
65. Stylli SS. Novel treatment strategies for glioblastoma. Cancers (Basel). 2020;12(10):2883.
66. Liu C, Ren L. Enhanced understanding of the involvement of ferroptosis in tumorigenesis: a review of recent research advancements. A Rev Recent Res Adv. 2023;3:37-48.
67. Candelli M, Franceschi F. New advances in gastroenterology: the crucial role of molecular medicine. Int J Mol Sci. 2023;24(19):14907.
68. Ciurea AV, Mohan AG, Covache-Busuioc RA, Costin HP, Glavan LA, Corlatescu AD, et al. Unraveling molecular and genetic insights into neurodegenerative diseases: advances in understanding alzheimer's, Parkinson's, and huntington's diseases and amyotrophic lateral sclerosis. Int J Mol Sci. 2023;24(13):10809.
69. Qin S, Xie B, Wang Q, Yang R, Sun J, Hu C, et al. New insights into immune cells in cancer immunotherapy: from epigenetic modification, metabolic modulation to cell communication. MedComm (2020). 2024;5(4):e551.
70. Ren S, Huang M, Bai R, Chen L, Yang J, Zhang J, et al. Efficient modulation of exon skipping via antisense circular RNAs. Research (Wash D C). 2023;6:0045.

71. Zhao H, Ding R, Han J. Ginsenoside Rh4 facilitates the sensitivity of renal cell carcinoma to ferroptosis via the NRF2 pathway. Arch Esp Urol. 2024;77(2):119-28.
72. Tian Z, Liu J, Zeng M, Zeng Q. Tong jing yi Hao formula alleviates ornidazole-induced oligoasthenospermia in rats by suppressing ROS/MAPK/HIF-1 pathway. Arch Esp Urol. 2023;76(8):596-604.
73. Liu Q, Long Q, Zhao J, Wu W, Lin Z, Sun W, et al. Cold-induced reprogramming of subcutaneous white adipose tissue assessed by single-cell and single-nucleus RNA sequencing. Research (Wash D C). 2023;6:0182.
74. Zhong M, Lee GM, Sijbesma E, Ottmann C, Arkin MR. Modulating protein–protein interaction networks in protein homeostasis. Curr Opin Chem Biol. 2019;50:55-65.
75. Chen YC, Chen HH, Chen PM. Catalase expression is an independent prognostic marker in liver hepatocellular carcinoma. Oncologie. 2024;26:79-90.
76. Zeng S, Chen X, Yi Q, Thakur A, Yang H, Yan Y, et al. CRABP2 regulates infiltration of cancer-associated fibroblasts and immune response in melanoma. Oncol Res. 2024;32(2):261-72.
77. Kong YL, Wang HD, Gao M, Rong SZ, Li XX. LncRNA XIST promotes bladder cancer progression by modulating miR-129-5p/TNFSF10 axis. Discov Onc. 2024;15(1):65.
78. Di Bonito P, Di Sessa A, Licenziati MR, Corica D, Wasniewska M, Miraglia Del Giudice E, et al. Sex-related differences in cardiovascular risk in adolescents with overweight or obesity. Rev Cardiovasc Med. 2024;25(4):141.
79. Fareed A, Amir N, Ajaz H, Sohail A, Vaid R, Farhat S. Advances in BRAF-targeted therapies for non-small cell lung cancer: the promise of encorafenib and binimetinib. Int J Surg. 2024;110(3):1891-3.
80. Liang S, Xu X, Yang Z, Du Q, Zhou L, Shao J, et al. Deep learning for precise diagnosis and subtype triage of drug-resistant tuberculosis on chest computed tomography. MedComm (2020). 2024;5(3):e487.
81. Yao JY, Yang YL, Chen WJ, Fan HY. Exploring the therapeutic potential of Qi Teng Mai Ning recipe in ischemic stroke and vascular cognitive impairment. Tradit Med Res. 2024;9:57.
82. Gao S, Shi X, Yue C, Chen Y, Zuo L, Wang S. Comprehensive analysis of competing endogenous RNA networks involved in the regulation of glycolysis in clear cell renal cell carcinoma. Oncologie. 2024;26:587-602.
83. Zhang J, He J, Chen W, Chen G, Wang L, Liu Y, et al. Simultaneous inversion of particle size distribution, thermal accommodation coefficient, and temperature of in-flame soot aggregates using laser-induced incandescence. Oncologie. 2024;17:0.
84. Wan X, Jiang M, Madan S. Research progress of nanomedicine for tumor immunotherapy. Cancer Insight. 2024;3:37-48.
85. Yang H, Li C, Xie Q. Advances in the use of nanomaterials in tumour therapy: challenges and prospects. Cancer Insight. 2024;2:37-48.
86. Dong F, Zheng L, Yang G. Construction of a TF-miRNA-mRNA regulatory network for diabetic nephropathy. Arch Esp Urol. 2024;77(1):104-12.
87. Ahmed MG, Shaheen N, Shaheen A, Meshref M, Nashwan AJ, Nassar NA, et al. Outcomes of endovascular treatment alone or with intravenous alteplase in acute ischemic stroke Patients: a retrospective cohort study. Brain Hemorrhages. 2024;5:21-8.
88. Sheng T, Feng Q, Luo Z, Zhao S, Xu M, Ming D, et al. Effect of phase clustering bias on phase-amplitude coupling for emotional EEG. J Integr Neurosci. 2024;23(2):33.
89. Huang J, Lin W, Sun Y, Wang Q, He S, Han Z, et al. Quercetin targets VCAM1 to prevent diabetic cerebrovascular endothelial cell injury. Front Aging Neurosci. 2022;14:944195.
90. Wang Y, Zhao ZJ, Kang XR, Bian T, Shen ZM, Jiang Y, et al. lncRNA DLEU2 acts as a miR-181a sponge to regulate SEPP1 and inhibit skeletal muscle differentiation and regeneration. Aging (Albany NY). 2020;12(12):24033-56.
91. Sun Y, Luo Z, Chen Y, Lin J, Zhang Y, Qi B, et al. si-Tgfbr1-loading liposomes inhibit shoulder capsule fibrosis via mimicking the protective function of exosomes from patients with adhesive capsulitis. Biomater Res. 2022;26(1):39.
92. Seto E, Yoshida M. Erasers of histone acetylation: the histone deacetylase enzymes. Cold Spring Harb Perspect Biol. 2014;6(4):a018713.
93. Meunier D, Seiser C. Histone deacetylase 1. In: Verdin E, editor. Histone deacetylases. Totowa, NJ: Humana Press; 2006. p. 3-22.

94. Lo CC, McNamara JB, Melendez EL, Lewis EM, Dufault ME, Sanai N, et al. Nonredundant, isoform-specific roles of HDAC1 in glioma stem cells. JCI Insight. 2021;6(14):e149232.
95. Vargas-Sierra O, Hernández-Juárez J, Uc-Uc PY, Herrera LA, Domínguez-Gómez G, Gariglio P, et al. Role of SLC5A8 as a tumor suppressor in cervical cancer. Front Biosci (Landmark Ed). 2024;29(1):16.
96. Wahi A, Bishnoi M, Raina N, Singh MA, Verma P, Gupta PK, et al. Recent updates on nano-phyto-formulations based therapeutic intervention for cancer treatment. Oncol Res. 2024;32(1):19-47.
97. Ma X, Yang Q, Lin N, Feng Y, Liu Y, Liu P, et al. Integrated anti-vascular and immune-chemotherapy for colorectal carcinoma using a pH-responsive polymeric delivery system. J Control Release. 2024;370:230-8.
98. Hirukawa S, Olson KA, Tsuji T, Hu G. Neamine inhibits xenografic human tumor growth and angiogenesis in athymic mice. Clin Cancer Res. 2005;11(24 Pt 1):8745-52.
99. Kunadis E, Lakiotaki E, Korkolopoulou P, Piperi C. Targeting post-translational histone modifying enzymes in glioblastoma. Pharmacol Ther. 2021;220:107721.
100. Olzscha H, Sheikh S, La Thangue NB. Deacetylation of chromatin and gene expression regulation: a new target for epigenetic therapy. Crit Rev Oncog. 2015;20(1-2):1-17.
101. Cheng Z, Li S, Yuan J, Li Y, Cheng S, Huang S, et al. HDAC1 mediates epithelial–mesenchymal transition and promotes cancer cell invasion in glioblastoma. Pathol Res Pract. 2023;246:154481.
102. Guo R, Li G, Guo Y. Hypertensive-like reaction: a definition for normotensive individuals with symptoms associated with elevated blood pressure. CVIA. 2022;6:6.
103. Wu Z, Chen S, Wang Y, Li F, Xu H, Li M, et al. Current perspectives and trend of computer-aided drug design: a review and bibliometric analysis. Int J Surg. 2024;110(6):3848-78.
104. Lin WJ, Shi WP, Ge WY, Chen LL, Guo WH, Shang P, et al. Magnetic fields reduce apoptosis by suppressing phase separation of tau-441. Research (Wash D C). 2023;6:0146.
105. Hong W, Lei H, Peng D, Huang Y, He C, Yang J, et al. A chimeric adenovirus-vectored vaccine based on Beta spike and Delta RBD confers a broad-spectrum neutralization against Omicron-included SARS-CoV-2 variants. MedComm (2020). 2024;5(4):e539.
106. Chu YM, Huang QY, Wang TX, Yang N, Jia XF, Shi ZM, et al. Actinidia chinensis Planch. root extract downregulates the Wnt/β-catenin pathway to treat gastric cancer: a mechanism study based on network pharmacology. Tradit Med Res. 2023;8:40.
107. Wang FC, Han P, Li H, Ye HY, Zhou PX, Tian W, et al. Advantages and prospects of traditional Chinese medicine in treating COVID-19. Tradit Med Res. 2023;8:22.
108. Wu H, Wang F, Yang L, Chen L, Tang J, Liu Y, et al. Carboxymethyl chitosan promotes biofilm-formation of Cryptococcus laurentii to improve biocontrol efficacy against Penicillium expansum in grapefruit. Adv Compos Hybrid Mater. 2024;7:23.
109. Botero DR. Paromomycin as effective treatment of taenia infections. Am J Trop Med Hyg. 1970;19(2):234-7.
110. Liu FY, Liu YF, Yang Y, Luo ZW, Xiang JW, Chen ZG, et al. SUMOylation in neurological diseases. Curr Mol Med. 2017;16(9):893-9.
111. Romano G. The complex biology of the receptor for the insulin-like growth factor-1. Drug News Perspect. 2003;16(8):525-31.
112. Dyer AH, Vahdatpour C, Sanfeliu A, Tropea D. The role of Insulin-Like Growth Factor 1 (IGF-1) in brain development, maturation and neuroplasticity. Neuroscience. 2016;325:89-99.
113. Zhang J, Huang FF, Wu DS, Li WJ, Zhan HE, Peng MY, et al. SUMOylation of insulin-like growth factor 1 receptor, promotes proliferation in acute myeloid leukemia. Cancer Lett. 2015;357(1):297-306.
114. Chen Y, Chen X, Luo Z, Kang X, Ge Y, Wan R, et al. Exercise-induced reduction of IGF1R sumoylation attenuates neuroinflammation in APP/PS1 transgenic mice. J Adv Res. 2024;69:279-97.
115. Chen Y, Fan Z, Luo Z, Kang X, Wan R, Li F, et al. Impacts of Nutlin-3a and exercise on murine double minute 2–enriched glioma treatment. Neural Regen Res. 2025;20(4):1135-52.
116. Chen Y, Huang L, Luo Z, Han D, Luo W, Wan R, et al. Pantothenate-encapsulated liposomes combined with exercise for effective inhibition of CRM1-mediated PKM2 translocation in Alzheimer's therapy. J Control Release. 2024;373:336-57.
117. McGee SL, Howlett KF, Starkie RL, Cameron-Smith D, Kemp BE, Hargreaves M. Exercise increases nuclear AMPK alpha2 in human skeletal muscle. Diabetes. 2003;52(4):926-8.
118. Jackson SE, Chester JD. Personalised cancer medicine. Int J Cancer. 2015;137(2):262-6.

119. Li T, Feng W, Yan W, Wang T. From metabolic to epigenetic: insight into trained macrophages in atherosclerosis (Review). Mol Med Rep. 2024;30(3):145.
120. Lan Y, Tian F, Tang H, Pu P, He Q, Duan L. Food therapy of scutellarein ameliorates pirarubicin-induced cardiotoxicity in rats by inhibiting apoptosis and ferroptosis through regulation of NOX2-induced oxidative stress. Mol Med Rep. 2024;29(5):84.
121. Yin T, Mou S, Zhang H, Dong Y, Yan B, Huang W, et al. CXCL10 could be a prognostic and immunological biomarker in bladder cancer. Discov Onc. 2024;15(1):148.
122. Wu C, Zhu X, Dai Q, Chu Z, Yang S, Dong Z. SUMOylation of SMAD4 by PIAS1 in conjunction with vimentin upregulation promotes migration potential in non-small cell lung cancer. Front Biosci (Landmark Ed). 2023;28(8):192.
123. Abuaisheh A, Aboud O. Biogenic amines in gliomas: a comprehensive literature review. Front Biosci (Landmark Ed). 2023;28(7):141.
124. Cui J, Shen W, Zhao H. New insights into extracellular vesicles between adipocytes and breast cancer orchestrating tumor progression. Front Biosci (Landmark Ed). 2023;28(6):129.
125. Guo Q, Du A, Wang J, Wang L, Zhu X, Yue X, et al. Integrated bioinformatic analyses reveal immune molecular markers and regulatory networks for cerebral ischemia-reperfusion. Front Biosci (Landmark Ed). 2023;28(8):179.